Theoretical Study of the CO Migratory Insertion Reactions of Pt(Me)(OMe)(dppe) and Ni(Me)(OR)(bpy) (R = Me, O-*p*-C_6H_4CN): Comparison of Group 10 Metal−Alkyl, −Alkoxide, and −Aryloxide Bonds

Stuart A. Macgregor* and Greg W. Neave

School of Engineering and Physical Sciences, William H. Perkin Building, Heriot-Watt University, Edinburgh EH14 4AS, U.K.

Received September 3, 2003

We report the results of theoretical mechanistic studies on the alternative migratory insertion reactions of CO with the metal−oxygen and metal−carbon bonds of Pt(Me)(OMe)(dhpe) (dhpe = $H_2PCH_2CH_2PH_2$) and Ni(Me)(OR)(α-diimine) (R = Me, Ph, α-diimine = NH═CHCH═NH) as models for Pt(Me)(OMe)(dppe) (dppe = $Ph_2PCH_2CH_2PPh_2$) and Ni(Me)(O-*p*-C_6H_4CN)(bpy) (bpy = 2,2′-bipyridyl), respectively. With Pt(Me)(OMe)(dhpe) the methoxycarbonyl product, Pt(Me)(CO_2Me)(dhpe), is favored over the acyl alternative, Pt{C(O)Me}(OMe)(dhpe), by 13 kcal/mol. Two alternative pathways for methoxycarbonyl formation were located, both of which are initiated via displacement of a chelate arm to form two isomers of Pt(Me)(OMe)(CO)(η^1-$H_2PCH_2CH_2PH_2$) (**2a**, CO trans to OMe; **2b**, CO trans to Me). Subsequent CO migratory insertion into the Pt−OMe bond of **2b** yields the methoxycarbonyl product directly. Alternatively, isomerization of **2a** to a third isomer, **2c** (CO trans to phosphine), can occur, from which CO migratory insertion again produces the methoxycarbonyl species. This latter isomerization/migratory insertion process represents the lowest energy pathway. Alternative CO migratory insertion reactions involving the Pt−Me bonds of **2a**,**c** suffer from very high activation barriers. The **2a** to **2c** isomerization is unusual, as it involves transfer of OMe to phosphine to give a metallophosphorane intermediate, followed by OMe transfer back to the metal. The net result is a swapping of the positions of the OMe and phosphine ligands. The computed kinetic and thermodynamic preference for reaction with the Pt−OMe bond is consistent with the observed reactivity of Pt(Me)(OMe)(dppe). With the Ni(Me)(OR)(α-diimine) systems CO migratory insertion proceeds via five-coordinate CO adducts. When R = Me, insertion into the Ni−OMe bond is more accessible kinetically but the acyl product is slightly more stable by 3.5 kcal/mol. Introduction of the Ph substituent dramatically lowers the reactivity of the Ni−OR bond, with the acyl becoming the kinetically more accessible species and being 18.4 kcal/mol more stable than the phenoxycarbonyl alternative. The lower reactivity of the Ni−OPh bond arises primarily from the weak C−O bond in the phenoxycarbonyl product and accounts for the experimental preference for acyl formation in the reaction of Ni(Me)(O-*p*-C_6H_4CN)(bpy) with CO.

Downloaded by NAT LIB UKRAINE on July 3, 2009
Published on January 17, 2004 on http://pubs.acs.org | doi: 10.1021/om030590k

Introduction

Low-valent late-transition-metal−oxygen bonds are of interest because of their role in homogeneous catalysis.[1] Catalytic aryl ether synthesis is founded on the intermediacy of low-valent metal alkoxides,[2] and such species could also play an important role in the development of schemes for the functionalization of alkenes.[3] There is now an extensive experimental literature describing the organometallic chemistry of low-valent metal alkoxides and aryloxides, with C−O bond forming reductive elimination[2,4] and β-H elimination[5] as well as insertion reactions with unsaturated molecules such as CO[6−15] and alkenes[16] all being documented. We are

* To whom correspondence should be addressed. E-mail: S.A.Macgregor@hw.ac.uk.

(1) (a) Bryndza, H. E.; Tam, W. *Chem. Rev.* **1988**, *88*, 1163. (b) Fryzuk, M. D.; Montgomery, C. D. *Coord. Chem. Rev.* **1989**, *95*, 1. (c) Fulton, J. R.; Holland, A. W.; Fox, D. J.; Bergman, R. G. *Acc. Chem. Res.* **2002**, *35*, 44.

(2) (a) Muci, A. R.; Buchwald, S. L. *Top. Curr. Chem.* **2002**, *219*, 131. (b) Hartwig, J. F. *Angew. Chem., Int. Ed.* **1998**, *37*, 2046.

(3) Tani, K.; Kataoka, Y. In *Catalytic Heterofunctionalization*; Togni, A., Grützmacher, H., Eds.; Wiley-VCH: Weinheim, Germany, 2001.

(4) (a) Williams, B. S.; Goldberg, K. I. *J. Am. Chem. Soc.* **2001**, *123*, 2576. (b) Han, R.; Hillhouse, G. L. *J. Am. Chem. Soc.* **1997**, *119*, 8135.

(5) (a) Zhao, J.; Hesslink, H.; Hartwig, J. F. *J. Am. Chem. Soc.* **2001**, *123*, 7220. (b) Blum, O.; Milstein, D. *J. Organomet. Chem.* **2000**, *594*, 479. (c) Blum, O.; Milstein, D. *J. Am. Chem. Soc.* **1995**, *117*, 4582. (d) Bryndza, H. E.; Calabrese, J. C.; Marsi, M.; Roe, D. C.; Tam, W.; Bercaw, J. E. *J. Am. Chem. Soc.* **1986**, *108*, 4805. (e) Macgregor, S. A.; Sweeney, B. *New J. Chem.* **2000**, *24*, 855.

(6) Bryndza, H. E. *Organometallics* **1985**, *4*, 1686.

(7) (a) Kim, Y.-J.; Osakada, K.; Takenaka, A.; Yamamoto, A. *J. Am. Chem. Soc.* **1990**, *112*, 1096. (b) Kim, Y.-J.; Osakada, K.; Sugita, K.; Yamamoto, T.; Yamamoto, A. *Organometallics* **1988**, *7*, 2182. (c) Komiya, S.; Akai, Y.; Tanaka, K.; Yamamoto, T.; Yamamoto, A. *Organometallics* **1985**, *4*, 1130.

(8) Tóth, I.; Elsevier, C. J. *J. Chem. Soc., Chem. Commun.* **1993**, 529.

(9) Smith, G. D.; Hanson, B. E.; Merola, J. S.; Waller, F. J. *Organometallics* **1993**, *12*, 568.

10.1021/om030590k CCC: $27.50 © 2004 American Chemical Society
Publication on Web 01/17/2004

Downloaded by NAT LIB UKRAINE on July 3, 2009
Published on January 17, 2004 on http://pubs.acs.org | doi: 10.1021/om030590k

interested in using density functional calculations to model such reaction chemistry, and in this paper we focus on two particularly well-characterized examples of CO migratory insertion. With Pt(Me)(OMe)(dppe) (dppe = 1,2-bis(diphenylphosphino)ethane) CO inserts into the Pt−OMe bond,[6] while, in contrast, with Ni(Me)-(O-*p*-C_6H_4CN)(bpy) (bpy = 2,2′-bipyridyl) CO inserts into the Ni−Me bond.[7c] Both of these reactions have been the subject of experimental mechanistic studies, which have shown that they proceed via intramolecular CO migratory insertion. With Pt(Me)(OMe)(dppe) evidence for a preequilibrium interaction with CO was presented, with migratory insertion yielding the stable methoxycarbonyl product Pt(Me)(CO_2Me)(dppe). The reaction with Ni(Me)(O-*p*-C_6H_4CN)(bpy) also proceeds via an associative mechanism. In this case insertion is rapidly followed by reductive elimination of an ester, although an acyl intermediate was characterized spectroscopically at low temperature.

We have recently completed a general computational study of CO migratory insertion reactions with the M−Me and M−OMe bonds of group 10 M(Me)(OMe)-(PH_3)$_2$ model systems.[17] For the Ni system methoxycarbonyl formation was slightly favored thermodynamically, but the lowest energy pathway was for insertion into the Ni−Me bond. Upon descending the triad, both kinetic and thermodynamic parameters increasingly favor methoxycarbonyl formation, and this becomes clearly preferred with the Pt model system. These results can be understood in terms of M−OMe and M−Me homolytic bond strengths, balanced against the stronger C−O bond formed in the methoxycarbonyl compared to the C−C bond in the alternative acyl. Thus, for Ni, the M−Me bond is significantly stronger than the M−OMe bond, but migratory insertion with the latter remains marginally preferred due to the stronger C−O bond of the methoxycarbonyl. For Pt, M−Me and M−OMe bonds are of comparable strength, and so the stronger methoxycarbonyl C−O bond results in a clear preference for reaction with the M−OMe bond. The ability of the alkoxide ligand to utilize the oxygen lone pairs to participate in C···O bond formation while maintaining an interaction with the metal center was also identified as a key factor in lowering activation energies for reaction with M−OMe bonds.

In the present paper we extend this general study to the specific mechanisms of CO migratory insertion with Pt(Me)(OMe)(dppe) and Ni(Me)(O-*p*-C_6H_4CN)(bpy). The calculations will use Pt(Me)(OMe)(dhpe) (dhpe = $H_2PCH_2CH_2PH_2$, (1,2-diphosphinoethane) and Ni(Me)-(OR)(α-diimine) (α-diimine = NH═CHCH═NH; R = Me, Ph) as model systems. We aim to account for the greater reactivity toward CO of the Pt−alkoxide bond in Pt(Me)-(OMe)(dppe) compared to the Ni−aryloxide bond in Ni(Me)(O-*p*-C_6H_4CN)(bpy), and the two Ni species will allow us to compare low-valent Ni−alkoxide and −aryloxide bonds. In general, experiment suggests that M−aryloxides are less reactive than M−alkoxides,[7a,10] although the reasons for this remain unclear.

Computational Details

Calculations used the Amsterdam Density Functional program, ADF1999.[18] A triple-ζ-STO basis set was employed for Ni and Pt, while all other atoms were described by a double-ζ plus polarization STO basis set. The frozen-core approximation was employed for the 1s electrons of C and O, up to and including the 2p electrons of P and Ni and the 4f electrons of Pt. All geometry optimizations used the procedure developed by Versluis and Ziegler[19] and incorporated the gradient corrections due to Becke[20] (exchange) and Perdew[21] (correlation) as well as the quasi-relativistic corrections of Snijders and co-workers.[22] All stationary points were fully optimized with no symmetry constraints, and transition states were characterized using numerical frequency analyses[23] and shown to have a unique imaginary frequency corresponding to the expected process. The nature of the energy minima linked via a given transition state was then confirmed by first distorting the transition-state geometry forward and back along the unique imaginary eigenvector and then allowing the structure to relax to either reactant or product in subsequent geometry optimizations. Bond dissociation energies were computed by comparing the energies of the radical species produced by homolytic metal−ligand bond cleavage, fully optimized via spin-unrestricted calculations, against the energy of the full molecule.

Results

Migratory Insertion of CO with Pt(Me)(OMe)-(dhpe). The computed structure of Pt(Me)(OMe)(dhpe) (**1**) is compared with that determined crystallographically for Pt(Me)(OMe)(dppe)[5d] in Figure 1. The two structures show reasonable agreement for metal−ligand distances; however, some discrepancies do arise, probably due to the neglect of OMe/dppe steric interactions in our model system. For example, the computed O−Pt−C angle is 12° too large and the OMe ligand is computed to lie in the metal coordination plane (the true C−O−Pt−*cis*-P torsion angle is 28°). The very short C−O distance of 1.258(19) Å reported experimentally is also not reproduced, as the calculated distance is much longer at 1.407 Å. Late-transition-metal alkoxides often exhibit short C−O distances experimentally, typically within the range 1.33−1.37 Å. While our calculations are in better accord with these other data, they still overestimate the C−O distance, and the reasons

(10) Kapteijn, G. M.; Dervisi, A.; Verhoef, M. J.; van den Broek, M. A. F. H.; Grove, D. M.; van Koten, G. *J. Organomet. Chem.* **1996**, *517*, 123.
(11) Dockter, D. W.; Fanwick, P. E.; Kubiak, C. P. *J. Am. Chem. Soc.* **1996**, *118*, 4846.
(12) (a) Bennett, M. A.; Rokicki, A. *Organometallics* **1985**, *4*, 180. (b) Bennett, M. A.; Yoshida, T. *J. Am. Chem. Soc.* **1978**, *100*, 1750.
(13) Michelin, R. A.; Napoli, M.; Ros, R. *J. Organomet. Chem.* **1979**, *175*, 239.
(14) (a) Stang, P. J.; Zhong, Z. *Organometallics* **1992**, *11*, 1026. (b) Huang, T.-M.; You, Y.-J.; Yang, C.-S.; Tzeng, W.-H.; Chen, J.-T.; Cheng, M.-C. Wang, Y. *Organometallics* **1991**, *10*, 1020.
(15) Yasuda, H.; Choi, J.-C.; Lee, S.-C.; Sakakura, T. *Organometallics* **2002**, *21*, 1216.
(16) (a) Bennett, M. A.; Jin, H.; Li, S.; Rendina, L. M.; Willis, A. C. *J. Am. Chem. Soc.* **1995**, *117*, 8335. (b) Bryndza, H. E. *Organometallics* **1985**, *4*, 406.
(17) Macgregor, S. A.; Neave, G. W. *Organometallics* **2003**, *22*, 4547.
(18) Baerends, E. J.; Ellis, D. E.; Ros, P. *Chem. Phys.* **1973**, *2*, 41. (b) te Velde, G.; Baerends, E. J. *J. Comput. Phys.* **1992**, *99*, 84. (c) Fonseca Guerra, C.; Snijders, J. G.; te Velde, G.; Baerends, E. J. *Theor. Chem. Acta* **1998**, *99*, 391.
(19) (a) Versluis, L.; Ziegler, T. *Chem. Phys.* **1988**, *88*, 322. (b) Fan, L.; Ziegler, T. *J. Am. Chem. Soc.* **1992**, *114*, 10890.
(20) Becke, A. D. *Phys. Rev. A* **1988**, *38*, 3098.
(21) Perdew, J. P. *Phys. Rev. B* **1986**, *33*, 8822.
(22) (a) Snijders, J. G.; Baerends, E. J.; Ros, P. *Mol. Phys.* **1979**, *38*, 1909. (b) Ziegler, T.; Tschinke, V.; Baerends, E. J.; Snijders, J. G.; Ravenek, W. *J. Phys. Chem.* **1989**, *93*, 3050. (c) van Lenthe, E.; Baerends, E. J.; Snijders, J. G. *J. Chem. Phys.* **1993**, *99*, 4597.
(23) Fan, L. Ziegler, T. *J. Chem. Phys.* **1992**, *96*, 9005. (b) Fan, L.; Ziegler, T. *J. Chem. Phys.* **1992**, *96*, 6937.

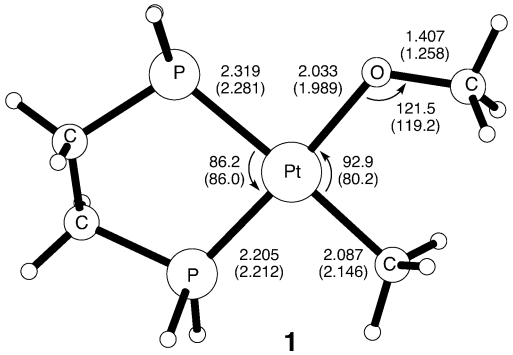

Figure 1. Selected computed geometric parameters (in Å and deg) for Pt(Me)(OMe)(dhpe) (**1**). Experimental data for Pt(Me)(OMe)(dppe)[5d] are given in parentheses for comparison.

for this and the particularly large discrepancy with the Pt(Me)(OMe)(dppe) system are not clear at this point.[24] Further calculations on $Pt(OMe)_2$(dhpe) as a model for $Pt(OMe)_2$(dppe)[5d] did give improved agreement for both Pt−O and C−O bonds (average distances are as follows: Pt−O, experimental 2.039(10) Å, computed 2.027 Å; C−O, experimental 1.370(19) Å, computed 1.411 Å).

Mechanistic studies on the reaction of Pt(Me)(OMe)(dppe) with CO suggest it proceeds through an initial five-coordinate CO adduct from which intramolecular migratory insertion can then occur. However, we found that computed reaction profiles for the approach of CO to **1** led to displacement of one of the chelating phosphine arms to give two isomers of Pt(Me)(OMe)(CO)(η^1-$PH_2CH_2CH_2PH_2$) (**2**). The more stable form (**2a**, $E = -12.8$ kcal/mol) has CO trans to OMe, while the second isomer (**2b**, $E = -4.2$ kcal/mol) has CO trans to Me (see Figure 2). These phosphine displacements are facile processes and proceed via low-energy trigonal-bipyramidal transition states ($\Delta E_{act} = +5.0$ kcal/mol via **1/2a-TS** for the formation of **2a** and +7.6 kcal/mol via **1/2b-TS** for **2b**). Experimentally, the evidence for a five-coordinate CO adduct was based on the retention in the NMR spectrum of ^{195}Pt coupling to both the ^{31}P phosphine and ^{1}H methoxide nuclei upon addition of CO to Pt(Me)(OMe)(dppe).[25] However, the formation of four-coordinate **2a** and **2b** can still be consistent with this picture if phosphine exchange is rapid on the NMR time scale. We find that for both **2a** and **2b** phosphine exchange can occur via trigonal-bipyramidal transition states with activation barriers of 13.4 and 13.3 kcal/mol, respectively, suggesting rapid phosphine exchange is possible. Cartesian coordinates for **1/2a-TS** and **1/2b-TS**, as well as these phosphine exchange transition states, are given in the Supporting Information.

Isomers **2a** and **2b** offer the possibility of CO migratory insertion with the Pt−Me and Pt−OMe bonds, respectively, and the stationary points for these processes are also shown in Figure 2. With **2a** migratory insertion into the Pt−Me bond proceeds with a large activation barrier of 28.0 kcal/mol via **2a-TS(C)** ($E = +15.2$ kcal/mol). With **2b** migratory insertion into the Pt−OMe bond is much more facile and proceeds via **2b-**

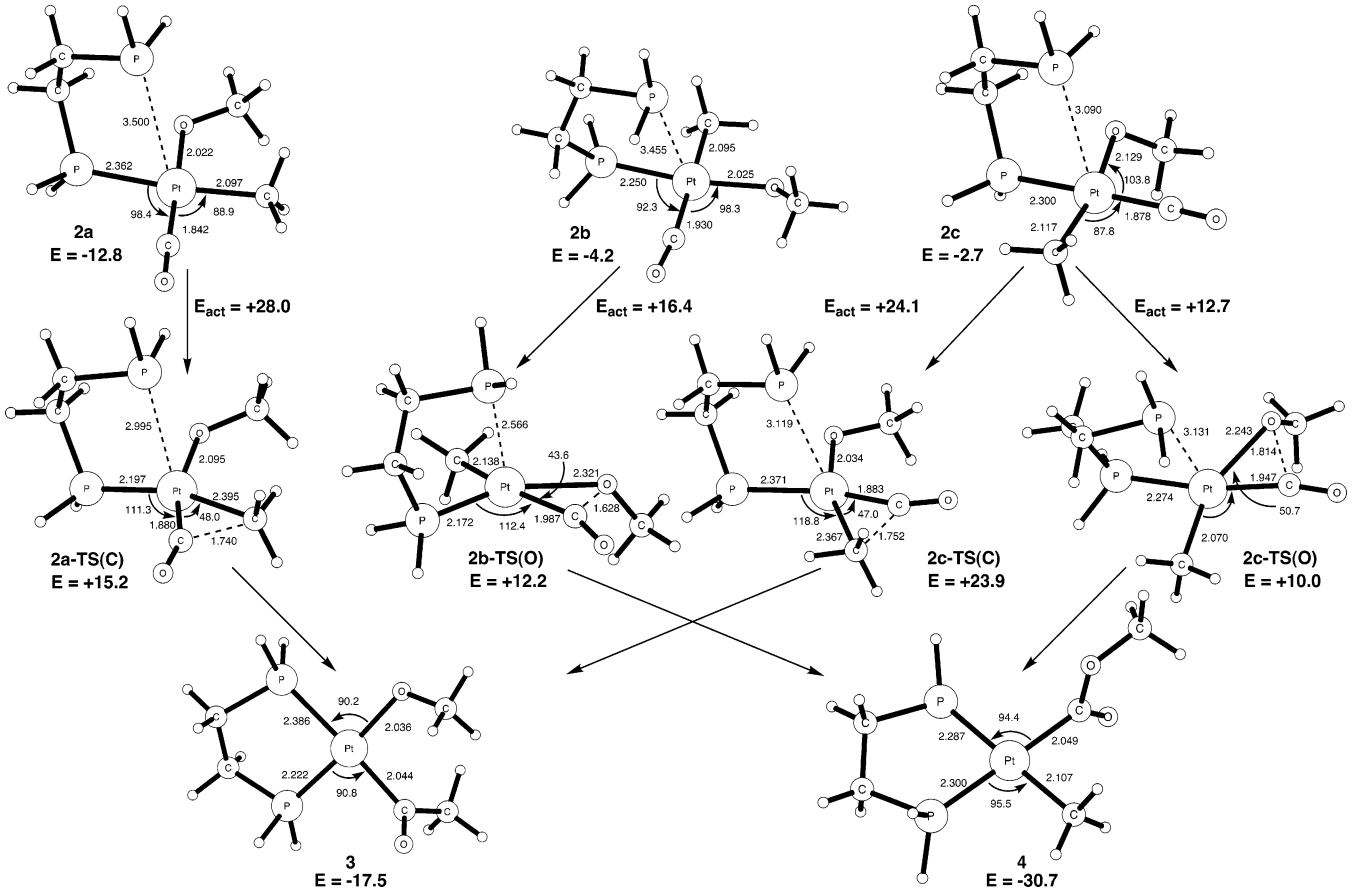

Figure 2. Selected computed geometric parameters (in Å and deg) and relative energies (in kcal/mol) for stationary points for the migratory insertion reactions of the isomers of Pt(Me)(OMe)(CO)(η^1-$PH_2CH_2CH_2PH_2$) (**2**). Energies are relative to **1** + free CO set to zero.

Downloaded by NAT LIB UKRAINE on July 3, 2009
Published on January 17, 2004 on http://pubs.acs.org | doi: 10.1021/om030590k

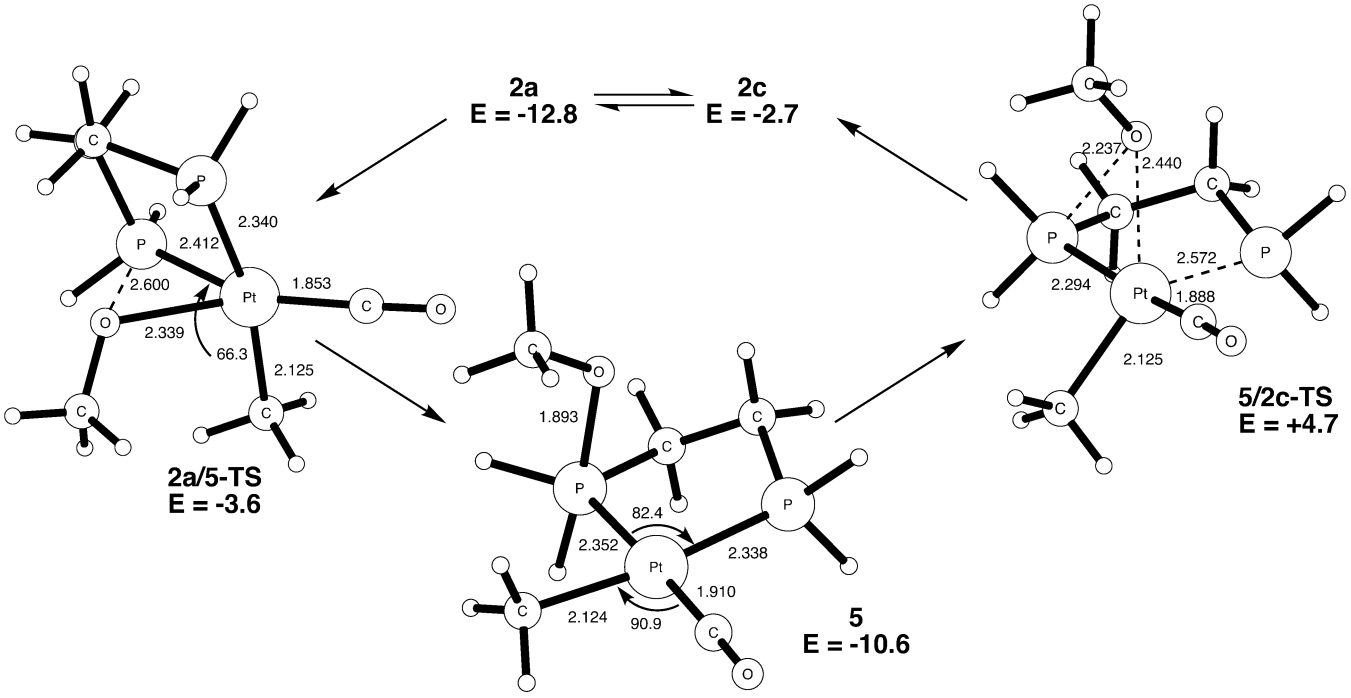

Figure 3. Selected computed geometric parameters (in Å and deg) and relative energies (in kcal/mol) for stationary points along the **2a** to **2c** isomerization pathway. Energies are relative to **1** + free CO set to zero.

Downloaded by NAT LIB UKRAINE on July 3, 2009
Published on January 17, 2004 on http://pubs.acs.org | doi: 10.1021/om030590k

TS(O) ($E = +12.2$ kcal/mol) with an activation energy of 16.4 kcal/mol. We have shown that the ability of the alkoxide ligand to utilize the oxygen lone pairs in C···O bond formation contributes to the lower activation energy for reaction with the Pt−OMe bond,[17] and the rotation of the methoxide ligand in **2b-TS(O)** is consistent with this effect. In comparison to the analogous reactions of the Pt(Me)(OMe)(CO)(PH_3) system studied previously, a reduction in activation energy is computed for both **2a** and **2b**. This is reflected in slightly earlier transition state structures in the present study and may be traced to the stabilizing influence of the remote phosphine group. From **2a** the Pt···P distance is reduced by 0.5 Å in forming **2a-TS(C)**, resulting in a small reduction in ΔE_{act} of 2 kcal/mol. From **2b** the Pt···P distance shortens by 0.9 Å to form **2b-TS(O)** and a more significant reduction in ΔE_{act} of 7 kcal/mol compared to the analogous Pt(Me)(OMe)(CO)(PH_3) reaction is computed. This is sufficient to make **2b-TS(O)** 3 kcal/mol more stable than **2a-TS(C)**. As these migratory insertion transition states are the highest energy points on the reaction profile from **1** + CO, there is therefore a kinetic preference for migratory insertion into the Pt−OMe bond via the intermediate **2b** and **2b-TS(O)**.

The initial products of migratory insertion were assessed by displacement of the transition-state geometries along their unique imaginary eigenvectors followed by optimization to a local minimum. From **2a-TS(C)** calculations did converge on a $T_{C(O)Me}$ three-coordinate acyl species, Pt{C(O)Me}(OMe)(η^1-$PH_2CH_2CH_2PH_2$) ($E = -1.8$ kcal/mol). However, a frequency calculation on this structure yielded two low-energy imaginary eigenvalues, and moving the remote phosphine arm slightly toward the metal and restarting the optimization resulted in this structure collapsing to the final four-coordinate migratory insertion product, Pt{C(O)Me}(OMe)(dhpe) (**3**; $E = -17.5$ kcal/mol). It is therefore unclear whether the three-coordinate acyl is a true minimum; however, the energy surface around this point is certainly very flat and any activation energy for phosphine arm recoordination will be minimal. In contrast, **2b-TS(O)** leads directly to the four-coordinate methoxycarbonyl product Pt(Me)(CO_2Me)(dhpe) (**4**; $E = -30.7$ kcal/mol). Methoxycarbonyl **4** is therefore 13.2 kcal/mol more favorable than acyl **3**, and so the migratory insertion of CO with the Pt−OMe bond of **1** is favored both thermodynamically and, via the formation of isomer **2b**, kinetically.

We have also considered the reactivity of a third form of Pt(Me)(OMe)(CO)(η^1-$PH_2CH_2CH_2PH_2$) (**2c**; $E = -2.7$ kcal/mol), in which CO is trans to phosphine. This isomer also presents the possibility of migratory insertion into the Pt−OMe bond, and the transition state for this process, **2c-TS(O)** ($E = +10.0$ kcal/mol), is in fact even more accessible than **2b-TS(O)** above (Figure 2). A transition state for migratory insertion into the Pt−Me bond of **2c**, **2c-TS(C)** ($E = +23.9$ kcal/mol), was also located but is much higher in energy. In **2c-TS(O)** and **2c-TS(C)** the remote phosphine arm is if anything further from the metal center than in **2c** and the activation energies are very similar to those found for the equivalent reactions of Pt(Me)(OMe)(CO)(PH_3). **2c-TS(O)** and **2c-TS(C)** were found to lead directly to the methoxycarbonyl and acyl products, respectively. Reaction through isomer **2c** therefore represents the lowest pathway for CO migratory insertion with the Pt−OMe bond of **1**, assuming that a low energy route for the

(24) The computed geometries were not significantly altered through use of either larger basis sets (ADF basis sets IV and V on the ligands) or the PW91 and BLYP functionals.

(25) We did initially search for five-coordinate forms of Pt(Me)(OMe)(CO)(dhpe) and located one species with both chelate arms and CO in equatorial positions ($E = -3.5$ kcal/mol). However, it is not clear how such a species could be formed directly from **1**. This five-coordinate species can be formed from **2c** by recoordination of the remote phosphine arm.

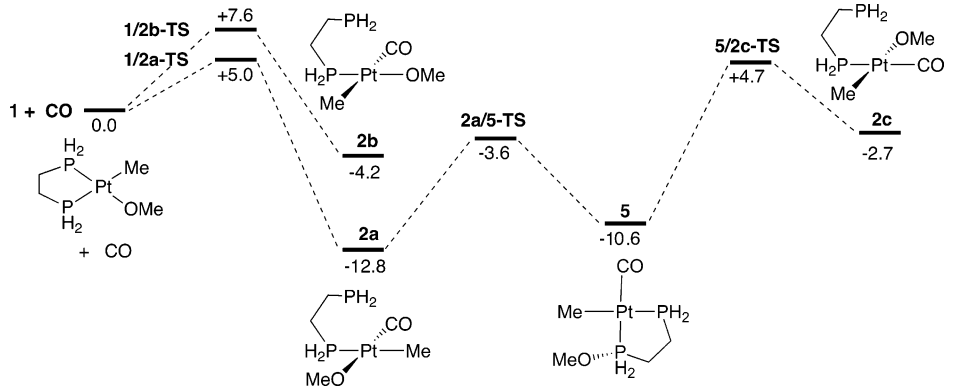

Figure 4. Computed reaction profiles (in kcal/mol) for the formation and interconversion of the isomers of **2**. Energies are relative to **1** + free CO set to zero.

formation of **2c** exists. As we have already found that CO addition to **1** leads only to isomers **2a** and **2b**, we focused on the possible isomerization processes of these latter species to give **2c**.[26]

In principle, isomerization between the forms of **2** may occur within both the four-coordinate and the five-coordinate regimes.[27] Appropriate four-coordinate square-planar−tetrahedral−square-planar processes could interconvert all the isomers of **2**; however, linear transits investigating such mechanisms involved prohibitively high energies. It is possible to write a five-coordinate isomerization pathway for the formation of **2c** from **2a** on the basis of a series of square-pyramidal species linked via trigonal-bipyramidal "transition states". Initial reaction profiles tracing the recoordination of the second phosphine arm in both **2a** and **2b** led to the phosphine exchange transition states discussed previously. Subsequent calculations also showed that no square-pyramidal structures exist as local minima. However, upon attempting to locate some of these species, we were struck by a marked elongation of the Pt−OMe bond as well as the movement of OMe ligand toward one arm of the chelating phosphine. Starting from one such geometry, a distorted-trigonal-bipyramidal transition state was located, which corresponded to the migration of OMe onto the (initially unbound) arm of the chelate of isomer **2a**. This transition state (**2a/5-TS**, $E = -3.6$ kcal/mol; see Figure 3) was found to link **2a** to a four-coordinate metallophosphorane featuring a phosphoranide ligand trans to CO (**5**, $E = -10.6$ kcal/mol). Overall, this reaction proceeds via initial recoordination of the phosphine arm onto the metal and then migration of OMe onto this phosphine.

Having established the possibility of the migration of OMe onto phosphine, the formation of **2c** from metallophosphorane **5** can be envisaged via a retro-migration process in which OMe is transferred back to the metal with displacement of the other phosphine arm. We were able to locate a transition state for this process (**5/2c-TS**, $E = +4.7$ kcal/mol), which thus completes the isomerization between **2a** and **2c**. **5/2c-TS** is the highest point on this isomerization pathway, which involves an overall activation energy relative to **2a** of 17.5 kcal/mol.

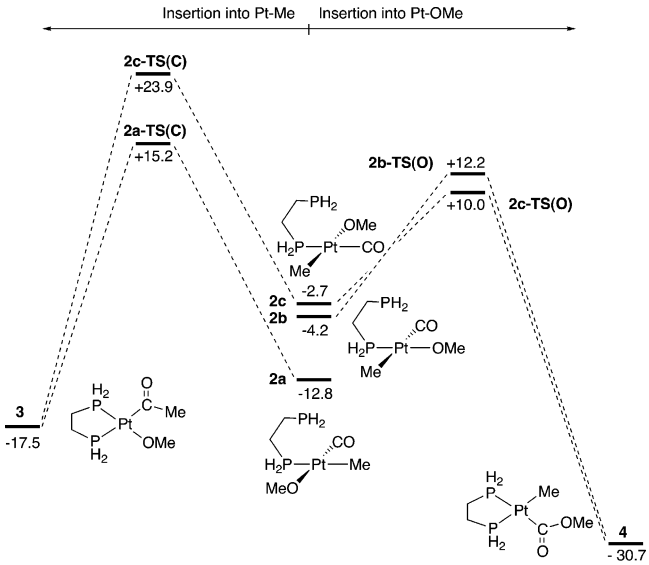

Figure 5. Computed reaction profiles (in kcal/mol) for the migratory insertion reaction of **1** with CO via the isomers of **2**. Energies are relative to **1** + free CO set to zero.

As **5/2c-TS** lies well below **2c-TS(O)**, the formation of isomer **2c** is kinetically accessible relative to any subsequent CO migratory insertion process. **2a/5-TS** and **5/2c-TS** both display distorted-trigonal-bipyramidal geometries, and their relative energies reflect the position of the CO ligand. In **2a/5-TS** CO is in the equatorial position, which stabilizes the structure, as this maximizes π-back-donation.[28] In **5/2c-TS** CO is in the less favorable axial position, and this structure is 8.3 kcal/mol higher than **2a/5-TS**.

The various processes for the formation and interconversion of the isomers of **2** are summarized in Figure 4, while the four reaction profiles for CO migratory insertion from the isomers of **2** are shown in Figure 5. In Figure 5 both transition states for reaction with the Pt−OMe bonds (**2b-TS(O)** and **2c-TS(O)**) are lower in energy than those for reaction with the Pt−Me bonds (**2a-TS(C)** and **2c-TS(C)**), and so two pathways are consistent with the greater kinetic reactivity of the Pt−OMe bonds. These are either initial formation of **2b** and direct reaction with the Pt−OMe bond, or initial formation of **2a**, isomerization to **2c**, and then reaction with the Pt−OMe bond.

(26) We thank Prof. C. J. Elsevier for emphasizing the importance of this isomerization process to us.

(27) We rejected the possibility of complete decoordination of the chelating phosphine to give a three-coordinate species, {Pt(CO)(Me)(OMe)}, which could itself then rearrange on the grounds of the highly unfavorable entropy that would be associated with chelate loss.

(28) Rossi, A. R.; Hoffmann, R. *Inorg. Chem.* **1975**, *14*, 365.

Downloaded by NAT LIB UKRAINE on July 3, 2009
Published on January 17, 2004 on http://pubs.acs.org | doi: 10.1021/om030590k

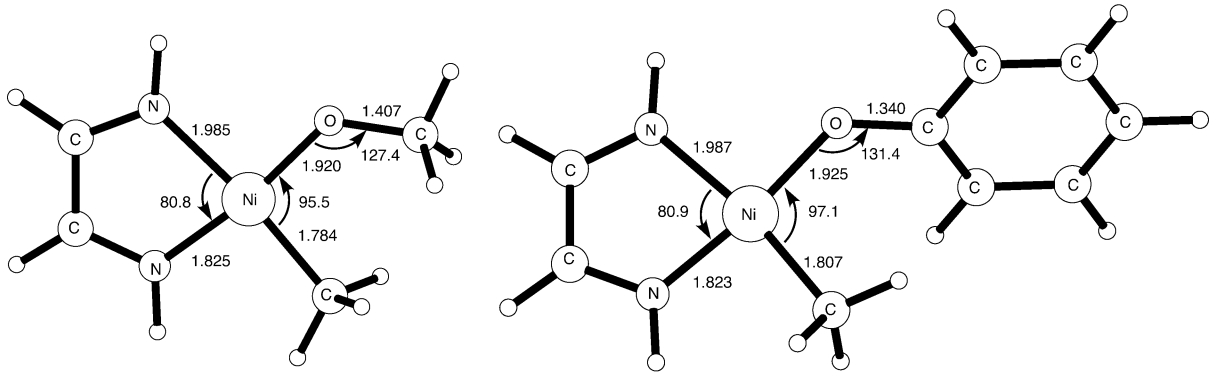

6 **7**

Figure 6. Selected computed geometric parameters (in Å and deg) for Ni(Me)(OMe)(α-diimine) (**6**) and Ni(Me)(OPh)(α-diimine) (**7**).

Migratory Insertion of CO with Ni(Me)(OR)(α-diimine) (R = Me, Ph). Calculations here aimed not only to model the reactivity of Ni(Me)(O-*p*-C_6H_4CN)(bpy), which displays a preference for migratory insertion of CO into the Ni−Me bond,[7c] but also to compare the reactivities of low-valent metal−alkoxide and −aryloxide bonds. The optimized structures of Ni(Me)(OMe)(α-diimine) (**6**) and Ni(Me)(OPh)(α-diimine) (**7**) are compared in Figure 6. The greater trans influence of the Me ligand is again evident in these structures, and both the Ni−O and Ni−C bonds are shorter than found previously for *cis*-Ni(Me)(OMe)-$(PH_3)_2$.[17] The major difference between **6** and **7** is the shorter C−O bond of the aryloxide. The computed value of 1.340 Å is in good agreement with crystallographic studies of group 10 aryloxides.[29]

Experimentally, the reaction between CO and Ni(Me)-(O-*p*-C_6H_4CN)(bpy) proceeds via a five-coordinate mechanism. Calculations screening for possible isomers of the five-coordinate Ni(Me)(OMe)(CO)(α-diimine) model intermediate, **8**, located three minima, trigonal-bipyramidal **8a** (E = −3.3 kcal/mol) and the two distorted-square-pyramidal isomers **8b** (E = −2.3 kcal/mol) and **8c** (E = +1.8 kcal/mol) (see Figure 7). **8a**,**b** can both be formed via CO addition to **6**, and reaction profiles indicate that both processes occur with minimal activation energies. The formation of **8c** can most easily be envisaged via isomerization of **8b**. However, we have not studied this process, as the reactivities of all three isomers are rather similar with, in each case, insertion into the Ni−OMe bond being favored kinetically (see Figure 7). Overall, the most accessible pathway involves reaction with the Ni−OMe bond of **8a** and the stationary points for the migratory insertion reactions of this species are shown in Figure 8.[30] **8a-TS(O)** is 4.6 kcal/mol more stable than the alternative acyl-forming transition state, **8a-TS(C)**, and rotation around the Ni−OMe bond in forming **8a-TS(O)** is again apparent. The acyl and methoxycarbonyl insertion products (**9** and **10**, respectively) are formed directly from **8a-TS(C)** and **8a-TS(O)** and exhibit standard geometries, with the large trans influence of the acyl group being evident in **9**. The product energies indicate a small preference for insertion into the Ni−Me bond ($\Delta\Delta E_R$ = 3.5 kcal/mol). Migratory insertion into the Ni−Me bond of **6** is therefore slightly favored thermodynamically, but the kinetic preference is for reaction with the Ni−OMe bond. This result is inconsistent with the low-temperature formation of an acyl product observed with Ni(Me)(O-*p*-C_6H_4CN)(bpy). In addition, this behavior is different from that found with the Ni(Me)(OMe)$(PH_3)_2$ model system, where the most accessible pathway was for acyl formation but the methoxycarbonyl product was favored thermodynamically.[17] For both model systems, however, alternative pathways and products are always close in energy (within 5 kcal/mol). Overall, the reactivity of mixed Ni−alkyl/methoxide systems appears to be subtly dependent on the nature of the metal coordination environment and it will be difficult to predict a priori their reaction selectivities.

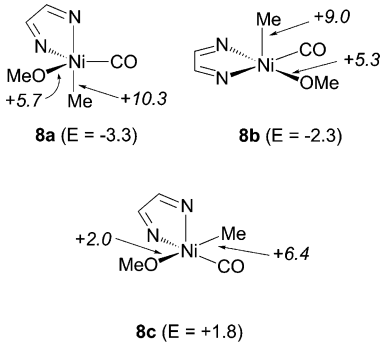

Figure 7. Schematic representations of the minima and relative energies (in kcal/mol) computed for Ni(Me)(OMe)-(CO)(α-diimine) (**8**). Numbers in italics are the computed activation energies for CO migratory insertion with the Ni−ligand bond indicated.

Due to the size of the system, we have limited our calculations on the CO migratory insertion with Ni(Me)-(OPh)(α-diimine) (**7**) to the most stable process computed for the OMe analogue, i.e., that involving Ni(Me)-(OPh)(CO)(α-diimine) (**11a**), the analogue of **8a** above. The major geometric difference between the OPh and OMe systems is seen in the transition states for reaction with the Ni−OR bonds, where a much later transition state structure is computed for the OPh system (Ni−O = 2.399 Å and O_{Me}−Ni−C_{CO} = 49.0° in **11a-TS(O)**; cf.

(29) (a) Kim, Y.-J.; Osakada, K.; Takenaka, A.; Yamamoto, A. *J. Am. Chem. Soc.* **1990**, *112*, 1096. (b) Braun, T.; Parsons, S.; Perutz, R. N.; Voith, M. *Organometallics* **1999**, *18*, 1710. (c) Holland, P. L.; Andersen, R. A.; Bergman, R. G.; Huang, J. Nolan, S. P. *J. Am. Chem. Soc.* **1997**, *119*, 12800. (d) Segilson, A. L.; Cowan, R. L.; Trogler, W. C. *Inorg. Chem.* **1991**, *30*, 3371. (e) Cámpora, J.; López, J. A.; Maya, C.; Palma, P.; Carmona, E.; Valerga, P. *J. Organomet. Chem.* **2002**, *643*, 331. (f) Holland, P. L.; Smith, M. E.; Andersen, R. A.; Bergman, R. G. *J. Am. Chem. Soc.* **1997**, *119*, 12815.

(30) Details of **8b** and **8c** and their related transition states are given as Supporting Information.

Downloaded by NAT LIB UKRAINE on July 3, 2009
Published on January 17, 2004 on http://pubs.acs.org | doi: 10.1021/om030590k

Downloaded by NAT LIB UKRAINE on July 3, 2009
Published on January 17, 2004 on http://pubs.acs.org | doi: 10.1021/om030590k

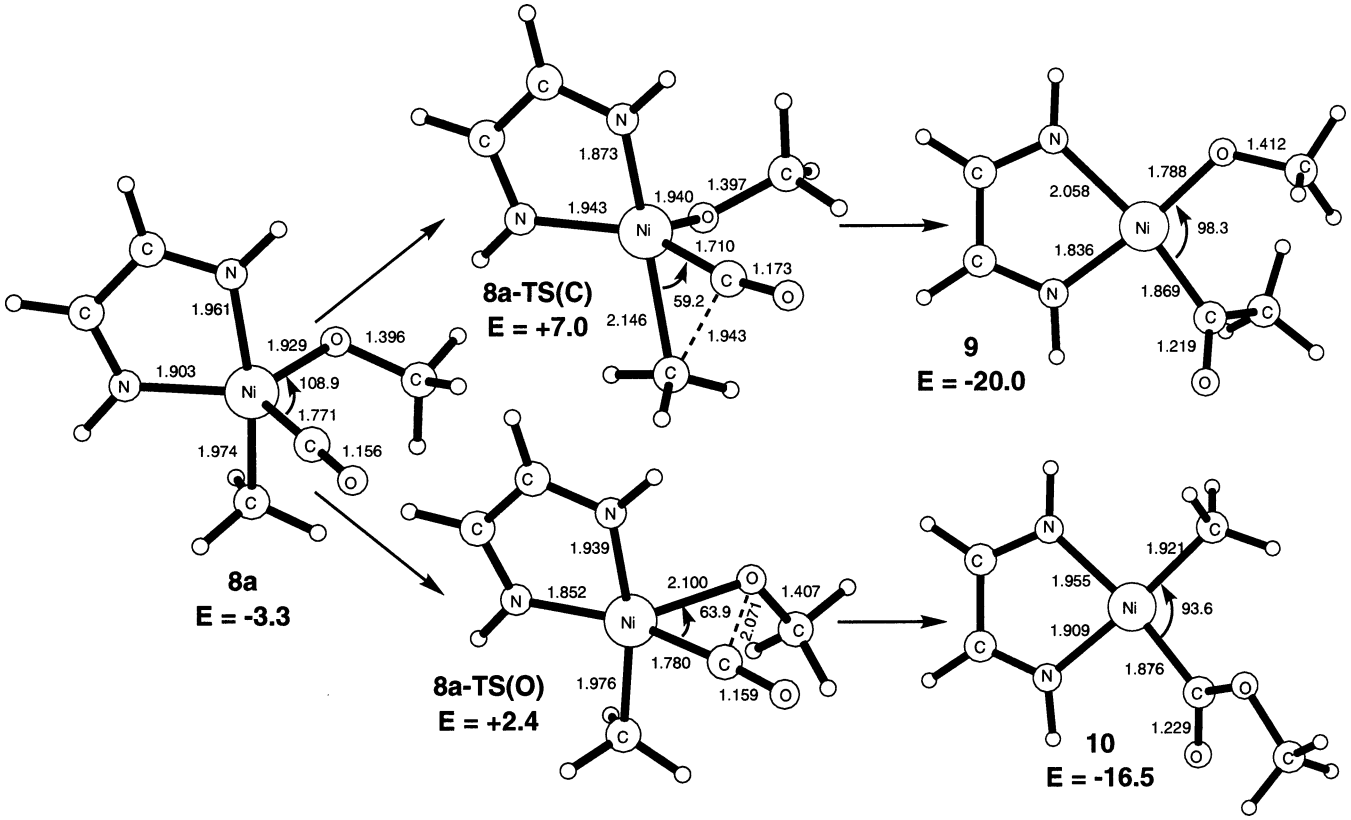

Figure 8. Selected computed geometric parameters (in Å and deg) and relative energies (in kcal/mol) for stationary points for the migratory insertion reactions of Ni(Me)(OMe)(α-diimine) (**6**) with CO via isomer **8a**. Energies are relative to **6** + free CO set to zero.

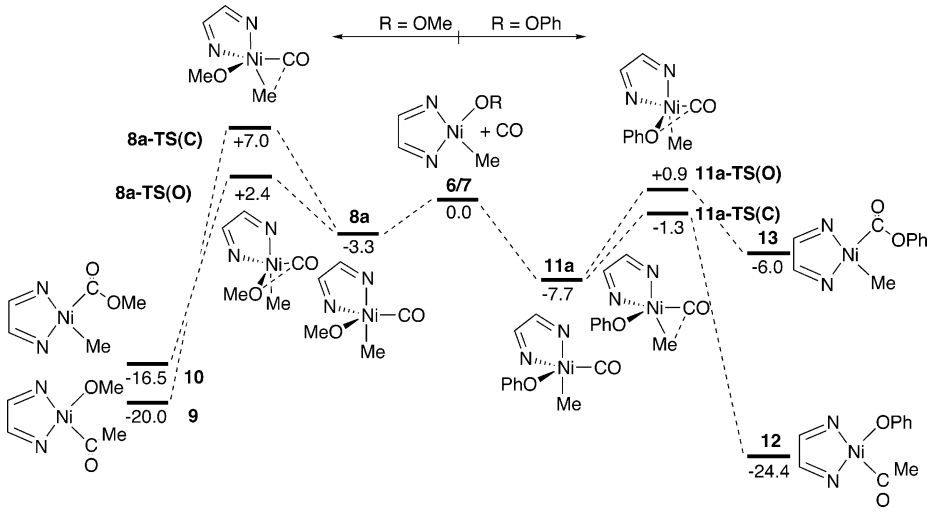

Figure 9. Computed reaction profiles (in kcal/mol) for the migratory insertion reactions of **6** and **7** with CO via five-coordinate **8a** and **11a**. Energies are relative to **6/7** + free CO set to zero.

2.100 Å and 63.9° in **8a-TS(O)** and see the Supporting Information for full details). This later geometry is reflected in a swapping of transition-state energies, with insertion into the Ni−Me bond now becoming favored. Even more significant are the changes in the relative energies of the acyl and aryloxy products, **12** and **13**, respectively. Figure 9 compares reaction profiles for CO migratory insertion with **6** and **7** and shows a strong thermodynamic preference for insertion into the Ni−Me bond of **7** ($\Delta\Delta E_R$ = 18.4 kcal/mol). Therefore, the introduction of the Ph substituent results in both a kinetic and thermodynamic preference for acyl formation. These results are now consistent with the observed behavior of Ni(Me)(O-*p*-C_6H_4CN)(bpy) and show the important role played by the aryl substituents in modulating the reactivity of M−OR bonds.[31]

Discussion

Reaction Mechanisms and Energetics. Two low-energy pathways have been located for the CO migratory insertion with the Pt−OMe bond of **1**. CO can

(31) We have also performed calculations with the O-*p*-C_6H_4CN substituent and find, compared to the OPh system, a slight increase in the kinetic and thermodynamic preference for reaction with the Ni−C bond ($\Delta\Delta E_{act}$ = 3.8 kcal/mol and $\Delta\Delta E_R$ = 21.4 kcal/mol, respectively).

Table 1. Computed Nickel−Ligand Homolytic Bond Dissociation Energies (kcal/mol) in Ni(Me)(OMe)(α-diimine) (6), Ni(Me)(OPh)(α-diimine) (7), Ni(Me)(CO_2R)(α-diimine) (10/13), and Ni{C(O)Me}(OR)(α-diimine) (9/12)

compd	Ni−ligand bond	energy
6	Ni−OMe	70.3
	Ni−Me	51.3
7	Ni−OPh	56.8
	Ni−Me	48.5
9	Ni−{C(O)Me}	52.4
10	Ni−CO_2Me	61.9
12	Ni−{C(O)Me}	54.1
13	Ni−CO_2Ph	63.2

displace the phosphine arm trans to Me to form **2b** and then insert directly into the Pt−OMe bond to give methoxycarbonyl **4**. Alternatively, CO can displace the phosphine arm trans to OMe to form **2a**, which then undergoes isomerization to give **2c** via metallophosphorane **5**. CO migratory insertion with the Pt−OMe bond of **2c** is the lowest energy pathway for the formation of **4**. These reaction pathways are much lower in energy than those computed for the formation of the acyl product, **3** via isomers **2a** and **2c**. In our earlier study on Pt(Me)(OMe)(PH_3)$_2$ we showed that the thermodynamic preference for insertion into the Pt−OMe bond arises not from differences in Pt−Me and Pt−OMe bond strengths but from the stronger C−O bond of the methoxycarbonyl product compared to the C−C bond of the alternative acyl. The same argument can be applied here, as the Pt−Me and Pt−OMe bonds in **1** again have similar homolytic bond strengths (64.7 and 67.1 kcal/mol, respectively). The relative strengths of the partially formed C···O and C···C bonds also play a role in stabilizing the Pt−OMe transition states, **2b-TS(O)** and **2c-TS(O)**, compared to the Pt−Me transition states, **2a-TS(C)** and **2c-TS(C)**. This effect is reinforced by the lone pair participation that is possible with the alkoxide ligand but not the alkyl.[17]

The CO migratory insertion reactions with the nickel species **6** and **7** proceed by CO addition to form five-coordinate intermediates and direct insertion into either the Ni−O or Ni−C bond. To account for the different reactivities of the nickel alkoxide **6** and the nickel aryloxide **7**, we have computed the relevant nickel−ligand homolytic bond strengths, and these are given in Table 1. When R = Me, the bond strength data suggest insertion into the Ni−Me bond will be favored, as the Ni−Me bond of **6** and the Ni−{C(O)Me} bond of **9** are of comparable strengths, whereas the Ni−OMe bond of **6** is 8.4 kcal/mol stronger than the Ni−CO_2Me bond in **10**. The fact that the computed thermodynamic preference for insertion into the Ni−Me bond of **6** is smaller than this ($\Delta\Delta E$ = 3.5 kcal/mol) reflects the stronger C−O bond formed in **10** compared to the C−C bond in **9**.[32] Comparing **6** and **7** shows the introduction of the phenyl substituent weakens the Ni−O bond by 13.5 kcal/mol, and on the basis of nickel−ligand bond strengths alone the two alternative migratory insertions derived from **7** should be approximately equally exothermic. As before, however, the C−O and C−C bonds that are formed in the alternative migratory insertion products are the key discriminating factors. We can gauge the strength of the new C(O)−O bond formed in **13** from the C(O)−O bond strength of phenyl acetate. This has been determined to be 76 kcal/mol,[33] 23 kcal/mol weaker than the C(O)−O bond in methyl acetate.[34] Assuming this trend is retained in **12** and **13**, the significant reduction in C(O)−O bond strength upon introduction of the Ph substituent also accounts for the much less thermodynamically favorable reaction with the Ni−OPh bond in **7** compared to the Ni−OMe bond in **6**. In contrast, the kinetics of migratory insertion are less affected by the nature of R. The barrier for insertion into Ni−OR is 3 kcal/mol higher when R = Ph compared to R = Me, and this may possibly be due to the lower nucleophilicity of the phenoxide lone pair. This effect, however, is relatively small.

Metallophosphorane Formation: Wider Implications in Catalysis? Although it is not necessary to invoke the **2a** to **2c** isomerization to account for the greater reactivity of the Pt−OMe bond of **1** (as **2b-TS(O)** is still lower in energy than either **2a-TS(C)** or **2c-TS(C)**), this isomerization process is interesting, as it involves the formation of a metallophosphorane, **5**, via OMe transfer from a metal to a phosphine. To date, all structurally characterized metallophosphoranes have featured cyclic phosphoranide ligands with at least two heteroatom substituents (N- or O-based) bound to phosphorus. **5** is therefore unusual, as it features both a noncyclic phosphoranide and has only one heteroatom substituent. The phosphoranide phosphorus center in **5** exhibits a distorted-trigonal-bipyramidal geometry with an axial OMe group, and the computed Pt−P distance agrees well with experimentally determined values for platinaphosphoranes with O-substituted phosphoranide ligands.[35]

There are several methods of metallophosphorane synthesis, the most general of which involve deprotonation of a parent phosphorane to form a reactive phosphoranide anion or nucleophilic attack of an electron-rich metal species at a phosphorane.[36] The novel intramolecular migration of OMe onto phosphine located in our calculations has not yet been reported in the experimental literature. However, such a process could be relevant to a number of catalytically important processes. Grushin and Alper have reported the key role of hydroxide in the reduction of $PdCl_2(PR_3)_2$ catalytic precursors to give active Pd^0 species.[37] This process is

(32) A similar rationale accounts for the different thermodynamic preferences exhibited by Ni(Me)(OMe)(α-diimine) (acyl formation) and Ni(Me)(OMe)(PH_3)$_2$ (methoxycarbonyl formation).[17] In Ni(Me)(OMe)(PH_3)$_2$ for methoxycarbonyl formation the Ni−OMe bond broken (60.5 kcal/mol) is comparable in strength to the Ni−CO_2Me bond formed (60.2 kcal/mol). For acyl formation a Ni−Me bond is broken (40.7 kcal/mol) and a Ni−C(O)Me bond is formed (43.7 kcal/mol). In terms of metal−ligand bond strengths, therefore, insertion into the Ni−Me bond should be favored by 3.3 kcal/mol. The fact that methoxycarbonyl formation is preferred with Ni(Me)(OMe)(PH_3)$_2$ (by 2.8 kcal/mol) can again be understood in terms of the stronger C−O bond formed compared to the C−C bond formed in the acyl.

(33) Carson, A. S.; Fine, D. H.; Gray, P.; Laye, P. G. *J. Chem. Soc. B* **1971**, 1611.

(34) *CRC Handbook of Chemistry and Physics*; Weast, R. C., Ed.; CRC Press: Boca Raton, FL, 1981.

(35) (a) Kajiyama, K.; Hirai, Y.; Otsuka, T.; Yuge, H.; Miyamoto, T. K. *Chem. Lett.* **2000**, *29*, 784. (b) Toyota, K.; Yamamoto, Y.; Akiba, K. *J. Chem. Res. S* **1999**, 386.

(36) (a) Dillon, K. B. *Chem. Rev.* **1994**, *94*, 1441. (b) Faw, R.; Montgomery, C. D.; Rettig, S. J.; Shurmer, B. *Inorg. Chem.* **1998**, *37*, 4136. (c) Kajiyama, K.; Nakamoto, A.; Miyazawa, S.; Miyamoto, T. K. *Chem. Lett.* **2003**, *32*, 332. (d) Toyota, K.; Yamamoto, Y.; Akiba, K. *J. Organomet. Chem.* **1999**, *586*, 171. (e) Lattman, M.; Morse, S. A.; Cowley, A. H.; Lasch, J. G.; Norman, N. C. *Inorg. Chem.* **1985**, *24*, 1364.

(37) Grushin, V. V.; Alper, H. *Organometallics* **1993**, *12*, 1890.

Downloaded by NAT LIB UKRAINE on July 3, 2009
Published on January 17, 2004 on http://pubs.acs.org | doi: 10.1021/om030590k

Scheme 1

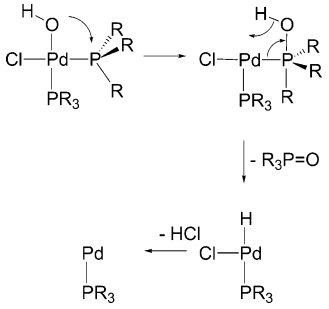

postulated to proceed via initial Cl^-/OH^- substitution followed by loss of phosphine oxide and HCl. Crucially, use of a chiral phosphine revealed that the phosphine oxide was formed with retention of configuration at P, ruling out an intermolecular S_N2-type displacement of L_nPd by OH^-. Instead, we suggest that an intramolecular migration of OH^- onto PR_3 of the type characterized here to give an intermediate metallophosphorane, followed by H-transfer, possibly to the metal, would be consistent with the observed stereochemical outcome (Scheme 1).

Although the transfer of heteroatom groups is without precedent, there are several examples of the transfer of hydrocarbyl groups between a phosphoranide ligand and a metal center. Riess and co-workers have studied the migrations of both phenyl and allyl groups in iron phosphoranides.[38] Very recently, a similar transfer of a naphthyl substituent in an Ir phosphoranido complex has been characterized.[36c] By analogy, one could consider that metallophosphoranes may potentially play a role as intermediates in unwanted aryl group exchange reactions in catalysis (Scheme 2).

The mechanism of such processes has been studied by Grushin,[39] who formulated the intermediate as a tight ion pair involving a phosphonium cation. Presumably a metallophosphorane species would lie on the reaction path to such an ion pair, even if only as a transient species.

(38) (a) Vierling, P.; Riess, J. G.; Grand, A. *Inorg. Chem*. **1986**, *25*, 4144. (b) Vierling, P.; Riess, J. G. *Organometallics* **1986**, *5*, 2543.
(39) Grushin, V. V. *Organometallics* **2000**, *19*, 1888.

Scheme 2

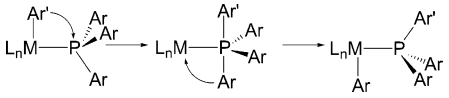

Conclusions

For Pt(Me)(OMe)(dhpe) (**1**), CO migratory insertion was found to be thermodynamically more favorable with the Pt−OMe bond by 13 kcal/mol. The reactions of **1** proceed through the phosphine-displaced intermediates **2a** and **2b** and insertion into the Pt−OMe bond is favored kinetically, either via **2b** or through a third isomer **2c** formed via isomerization of **2a**. **2a** to **2c** isomerization can proceed through a metallophosphorane, **5**. Both the thermodynamic and kinetic preference for insertion into the Pt−OMe bond are consistent with the observed reactivity of Pt(Me)(OMe)(dppe).

For the Ni(Me)(OR)(α-diimine) model systems **6** (R = Me) and **7** (R = Ph), migratory insertion proceeds via five-coordinate intermediates. With the methoxide species the kinetic preference is for insertion into the Ni−OMe bond, but a small thermodynamic preference for insertion into the Ni−Me bond is found. With R = Ph the kinetic preference is for insertion into the Ni−Me bond and a dramatic reduction in the exothermicity of the migratory insertion into the Ni−O bond is computed. The key factor in this case appears to be the weak C(O)−O bond formed in the phenoxycarbonyl product. The kinetic and strong thermodynamic preference for acyl formation is consistent with the observed reactivity of Ni(Me)(O-*p*-C_6H_4CN)(bpy).

Acknowledgment. We thank Dr. V. V. Grushin for useful discussions and the EPSRC and Heriot-Watt University for financial support.

Supporting Information Available: Tables of Cartesian coordinates and energies for all stationary points and unique imaginary eigenvalues for all transition states. This material is available free of charge via the Internet at http://pubs.acs.org.

OM030590K

Downloaded by NAT LIB UKRAINE on July 3, 2009
Published on January 17, 2004 on http://pubs.acs.org | doi: 10.1021/om030590k